

Fundamental Limits to Stereotactic Proton Therapy

Stephen G. Peggs

Abstract—Proton therapy techniques are developing from passive scattering towards 3-D multi-field scanning modalities, increasing the demands for speed and for dose distributions with sharp edges. Fundamental physics (energy straggling and multiple Coulomb scattering) ultimately limit treatment performance parameters, even for an ideal beam delivery system. This paper calculates how few independent beam delivery control points are needed in a tumor in order to perform the sharpest possible stereotactic surgery, with 1% integrated dose flatness.

Index Terms—Proton therapy, accelerator, treatment planning.

I. INTRODUCTION

MOST contemporary proton therapy beamlines use passive scattering nozzles, in which the incoming beam passes through a significant amount of matter in “beam spreaders”, just before entering the patient [1]. These spread the transverse profile of the beam, in order to deliver a broad and flat dose distribution to a tumor at the end of the proton beam range. They also inevitably increase the energy spread of the beam, resulting in a broader range distribution. Fixed energy proton sources (such as cyclotrons) also require “energy degraders” in the beam, to independently tune the average energy (and range) of the beam delivered to the patient.

Some advanced beamlines use active scanning techniques to deliver a radiation dose that conforms much more closely to the lateral contours of the tumor. Figure 1a shows how the total dose to the patient is built up in many “range layers”, each corresponding to one particular average beam energy. The beam is scanned laterally in two dimensions by adjusting steering magnets, to best fit the outline of the tumor at that depth. Then the energy is reduced slightly, and the next energy layer is scanned. Conformal treatment succeeds because there is less material in the beamline – the lateral and longitudinal dose distributions are much narrower for each beam delivery. The oncologists “knife” is much sharper in active scanning, within limits that apply even for a perfect proton source.

This paper assumes that a perfect incoming beam has negligible energy spread and emittance (lateral size), regardless of whether the proton source is a cyclotron or a synchrotron, extraction is fast or slow, et cetera. The sharpness of the knife is then limited by the physics of proton passage through matter; Figure 1b illustrates how energy straggling leads to a finite range spread and a blurry Bragg peak for a single beam delivery, while multiple Coulomb scattering broadens the beam.

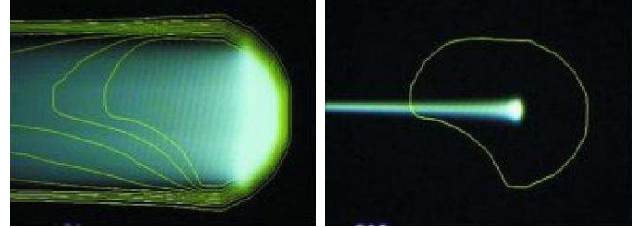


Fig. 1. Lateral scanning at multiple range layers [2]. a) The integrated dose is built up layer by layer. b) Energy straggling and multiple Coulomb scattering blur the single beam delivery dose longitudinally and laterally.

Active scanning can be performed in various ways. A continuous beam from a cyclotron, or slowly extracted beam from a synchrotron, may pause at a sequence of control points in each energy layer, quickly moving to the next point when enough local dose has been accumulated. Alternatively, fast extracted beam pulses can be delivered to each control point, one after the other. In many clinical cases the dose distribution is enhanced if beam is delivered to the same set of control points from more than one direction, or “field”. Some facilities choose to pass over the same set of control points multiple times.

This paper avoids such scanning implementation details by asking a simple question: “How few independent control points are needed to perform the sharpest possible stereotactic surgery with 1% integrated dose flatness, limited only by the physics of proton interactions with matter?” An accurate answer for a particular tumor depends on its detailed geometry, requiring the thorough application of a treatment planning system. The approximate answer given below for a simple prism geometry is nonetheless instructive, for example in the way that it scales with tumor volume. The answer is relatively insensitive to the required dose flatness, justifying the use of a value of 1% that is smaller than the currently commonplace values of 3% or more.

A. Straggling and multiple Coulomb scattering

Protons deposit much of their dose in a Bragg peak at the end of their range. The individual Bragg peak widths in Figure 2 are due solely to energy straggling statistical fluctuations that accumulate as the protons traverse the patient. Figure 2 shows how a total dose distribution with 1% flatness accumulates at a depth of about 20 cm in water by scanning the beam energy in 3.4 MeV steps – much larger than the RMS energy width of about 1.4 MeV. Figure 3 shows how range straggle and maximum step size vary as function of penetration depth. Similarly, Figure 4 shows how multiple Coulomb scattering fluctuations cause significant transverse beam size growth, even for a beam with zero initial size. The results in Figures 2–5 are derived from simple analytical fits [3] to results from a Monte Carlo code [4] that contains all the important physics [5].

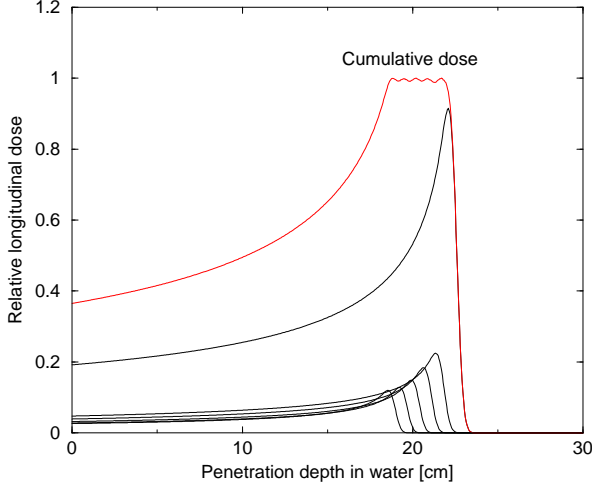


Fig. 2. Longitudinal dose versus depth, showing sharp Bragg peaks for each of 6 beam energies. After traversing about 20 cm of water the beam acquires an RMS energy width of about 1.4 MeV, due solely to energy straggling. Six incoming beam energies from 167.0 to 184.5 MeV correspond to 6 overlapping energy layers, which add to give a cumulative dose that is flat at the 1% level.

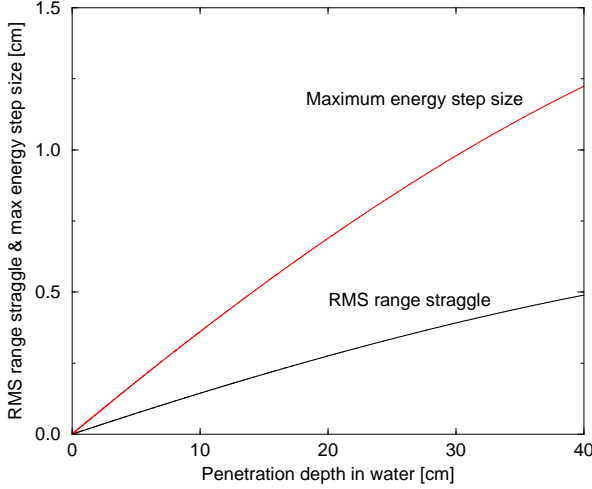


Fig. 3. Range straggling and the maximum spacing of energy layers. Because of the long dose tail upstream of the Bragg peak, it is possible to space the energy layers about 2.5 times further apart than the RMS range straggle, while maintaining 1% cumulative dose fitness.

II. VARIABLE FOCUSING NOZZLE

Figure 5 shows the transverse dose accumulated when a sequence of Gaussian beam deliveries of varying size and intensity overlap. If the spacing between the centers of deliveries b and $b + 1$ is set to be

$$x_{b+1} - x_b = 0.5 (\sigma_{b+1} + \sigma_b) \quad (1)$$

where σ_b is the RMS size of the b 'th delivery, then the accumulated transverse dose is flat to better than 1%. The total transverse beam size for each beam delivery, or pixel, is determined by adding in quadrature the multiple scattering beam size σ_{MS} and the optical beam size σ_{OPT}

$$\sigma_b^2 = \sigma_{MS}^2 + \sigma_{OPT}^2 \quad (2)$$

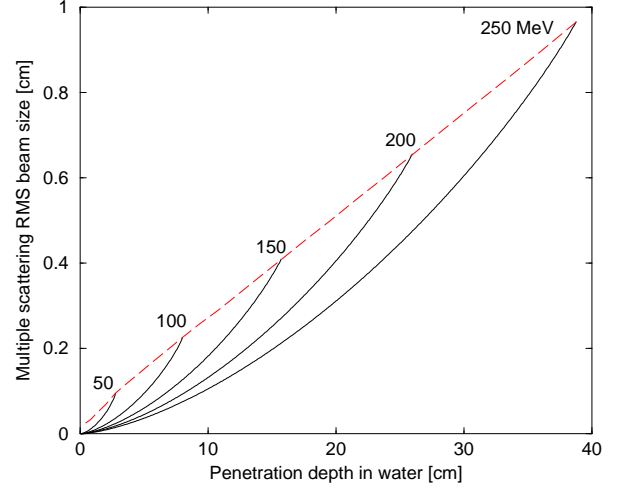


Fig. 4. Transverse proton beam size due to multiple Coulomb scattering. Although the beam enters with zero emittance, it acquires a near-Gaussian transverse beam distribution. For example, a beam with a range of about 20 cm accumulates an RMS size of $\sigma_{MS} \approx 0.5$ cm by the end of its range.

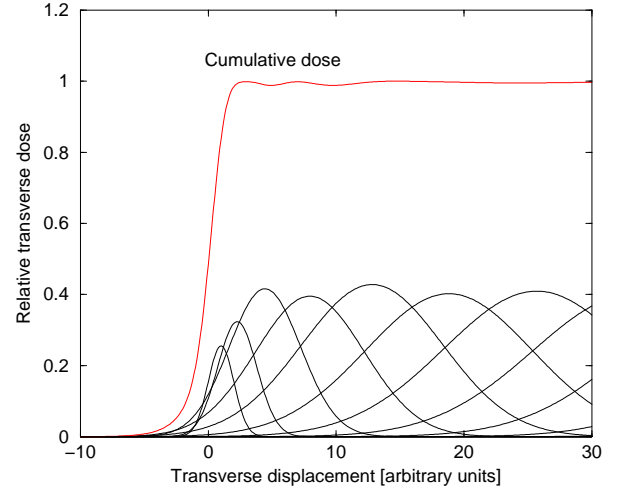


Fig. 5. Transverse dose profile from a sequence of overlapping Gaussian beam deliveries with empirically determined intensities. The sharp edge is achieved by delivering a minimum width (σ_{MS}) beam at the surface of the tumor. A cumulative dose fitness of 1% is achieved even while the beam size increases rapidly as a function of depth.

The optical beam size

$$\sigma_{OPT}^2 = \epsilon \beta \quad (3)$$

depends on both the unnormalized RMS emittance ϵ – the intrinsic size of the source beam – and the magnetic optical settings of the gantry and nozzle, represented by the “beta function” β at the tumor. Figure 6 shows two settings of a variable focusing nozzle that varies β over more than a factor of 100, varying σ_{OPT} over a dynamic range of more than 10. (This gantry and nozzle also provide a transverse scanning field of ± 20 cm [6].) It is necessary to be able to achieve

$$\sigma_{OPT} \ll \sigma_{MS} \quad (4)$$

in order to be able to achieve the smallest possible beam size. Thus the requirement on the beam delivery system is

$$\epsilon \beta_{MIN} \ll \sigma_{MS}^2 \quad (5)$$

For example, if $\sigma_{MS} = 0.5$ cm and $\beta_{MIN} = 1.0$ m, then it is necessary that $\epsilon \ll 25$ μm .

III. TUMOR PRISM MODEL

Figure 7 shows a tumor that has the same cross section throughout its entire depth of distance D – it is a prism. This simple geometry is straightforward to analyze. Different energy layers of the tumor are irradiated in sequence, by stepping the energy of the incoming beam. It is convenient to associate the area A and the perimeter C of each layer by introducing a form factor $f \geq 1$ through

$$C = f \sqrt{4\pi A} \quad (6)$$

This form factor measures the complexity of the convolutions around the perimeter of the layer, where the beam pixels are smallest. It attains the value of $f = 1$ only for a perfect circle.

Figure 8 schematically represents a small section of the perimeter, showing how overlapping chains of constant size pixels – contours – are superimposed. The pixel size increases for contours further from the edge of the layer, so that the total number of pixels within the “skin depth” is given by

$$N_{SKIN} = \sum_{b=0}^{b_S} \frac{C}{\sigma_b} \quad (7)$$

where b_S is the number of the contour at which the pixel size effectively reaches its maximum. This can be rewritten as

$$N_{SKIN} = \lambda_S \frac{C}{\sigma_{MS}} \quad (8)$$

where the dimensionless “integrated linear density”

$$\lambda_S = \sum_{b=0}^{b_S} \frac{\sigma_{MS}}{\sigma_b} \quad (9)$$

depends only on how fast the pixel sizes of successive contours converge to their final maximum value. The convenient form

$$N_{SKIN} \approx \left(\lambda_S f \sqrt{4\pi} \right) \frac{\sqrt{A}}{\sigma_{MS}} \quad (10)$$

is found by substituting Equation 6 into Equation 8.

In the interior core of the range layer there are approximately

$$N_{CORE} = \frac{A}{M^2 \sigma_{MS}^2} \quad (11)$$

pixels, where M is the dynamic range of the pixel size

$$M \equiv \frac{\sigma_{MAX}}{\sigma_{MS}} \quad (12)$$

The total number of pixels per energy layer is minimized if it is dominated by the number of small pixels that are inevitably required to give a sharp dose profile around the perimeter, when

$$N_{CORE} \ll N_{SKIN} \quad (13)$$

This condition is met if the dynamic range is large enough

$$M^2 \gg \frac{1}{\lambda_S} \frac{A}{C \sigma_{MS}} \quad (14)$$

Substituting Equation 6 into Equation 14 gives the alternate convenient form

$$M^2 \gg \left(\frac{1}{\lambda_S f \sqrt{4\pi}} \right) \frac{\sqrt{A}}{\sigma_{MS}} \quad (15)$$

This condition is not hard to meet in practice, as shown below.

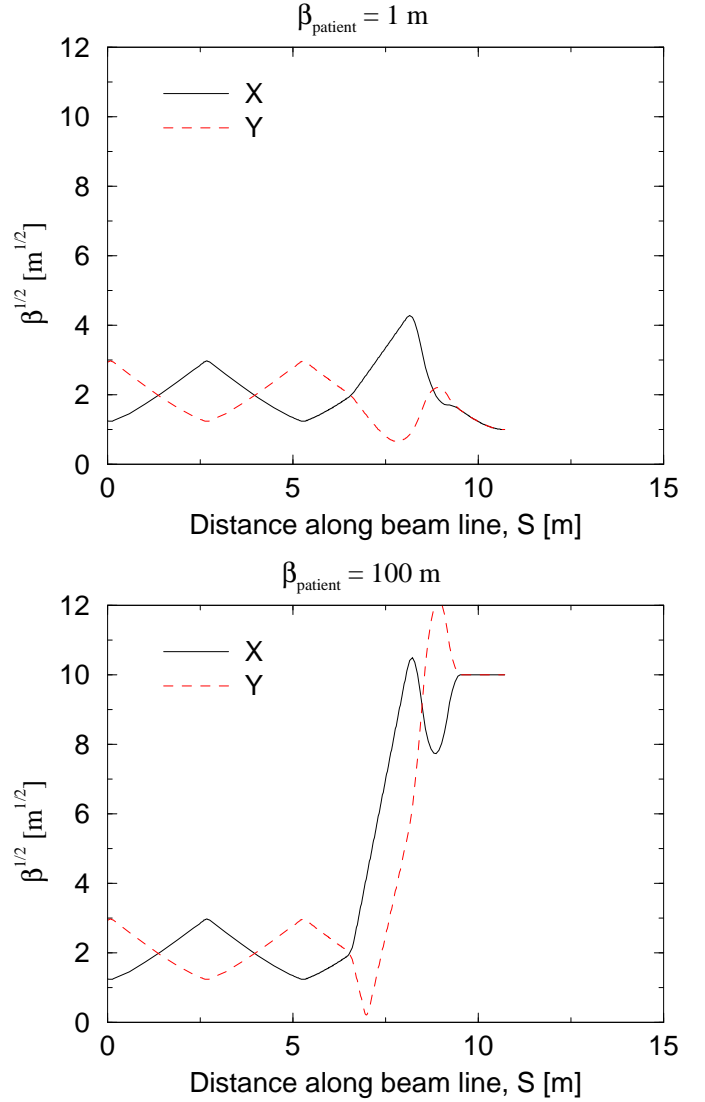


Fig. 6. Variable focusing nozzle optics can achieve a broad range of beam sizes at the patient. For example, varying β from 1 m to 100 m results in a dynamic range of 10 in σ_{OPT} , the beam size component due to the beam delivery system. The total beam size is found by adding this component in quadrature with the multiple scattering size, σ_{MS} .

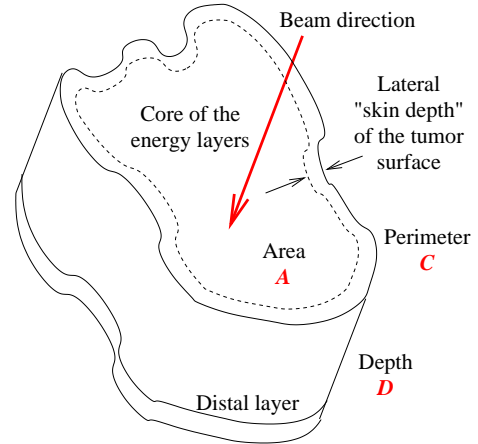


Fig. 7. Simple model of a tumor in the shape of a prism, with the same lateral cross section throughout the entire depth, D . The cross-sectional area is A , with a perimeter length C . The pixel size is significantly reduced inside the skin depth at the edge of each energy layer.

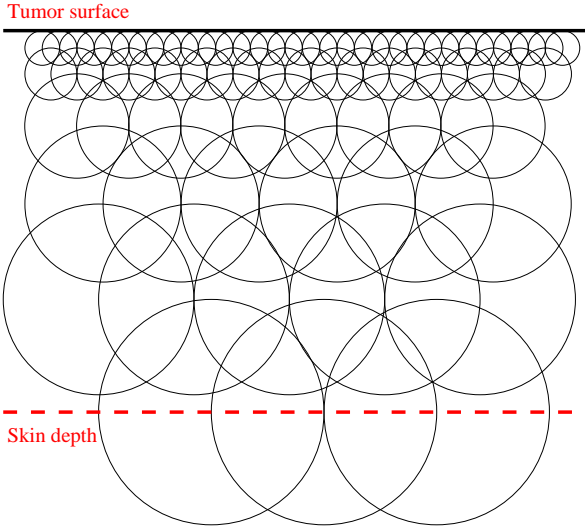


Fig. 8. Cartoon depiction of increasing pixel size at overlapping contours near the lateral edge – the tumor surface – in one particular range layer corresponding to one particular beam energy. The beam direction is into the page. The pixel size is close to its asymptotic value at the contour with index number $b_S = 5$, at the skin depth.

If the energy layers are uniformly spaced by Δ , then about

$$N_E = \frac{D}{\Delta} \quad (16)$$

different energies are required to scan the entire depth of the tumor. Thus the grand total of the number of control points, or voxels, required to irradiate the tumor is about

$$N_{TOT} = \lambda_S \frac{D C}{\Delta \sigma_{MS}} \quad (17)$$

This can also be written

$$N_{TOT} \approx \left(\lambda_S f \sqrt{4\pi} \right) \frac{D \sqrt{A}}{\Delta \sigma_{MS}} \quad (18)$$

in a more convenient form.

IV. A TYPICAL CONTOUR SIZE SERIES

One of many plausible contour size series is

$$\sigma_b = \sigma_{MS} \left(1 + (M-1) \frac{(b/b_0)^2}{1 + (b/b_0)^2} \right) \quad (19)$$

as shown in Figure 9a. Figure 5 demonstrates that this series results in an accumulated dose profile with 1% flatness when the knee of the series $b_0 = 4$ and the dynamic range of the pixel size is $M = 10$. In this case Figure 9b shows that the skin depth is effectively

$$b_S = 5 \quad (20)$$

resulting in an integrated linear density of

$$\lambda_S = 2.6 \quad (21)$$

Thus the approximate number of pixels in each energy layer is

$$N_{SKIN} \approx 9.2 f \frac{\sqrt{A}}{\sigma_{MS}} \quad (22)$$

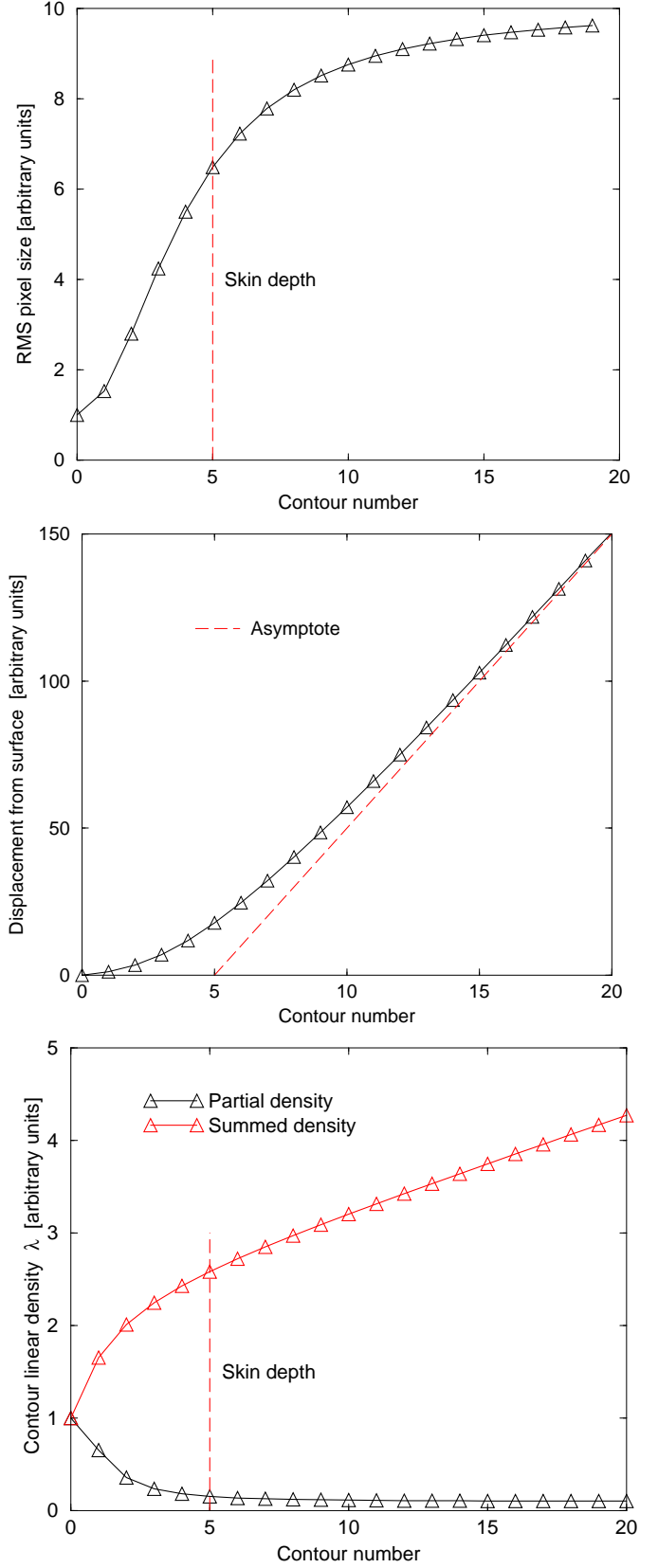


Fig. 9. Lateral contour distributions. a) Pixel size increases by a factor of 10 for deep contours. b) The effective skin depth boundary is at contour $b_S = 5$. c) Linear density of pixels versus contour number. The accumulated linear density is $\lambda_S = 2.6$ at the skin depth.

if the condition for the number of pixels in the core to be negligible

$$M^2 \gg \frac{0.11}{f} \frac{\sqrt{A}}{\sigma_{MS}} \quad (23)$$

is met. In this case the total number of voxels required is

$$N_{TOT} \approx 9.2 f \frac{D \sqrt{A}}{\Delta \sigma_{MS}} \quad (24)$$

It is interesting to evaluate these quantities in a numerical example.

V. LARGE AND SMALL TUMORS

Suppose that a tumor prism has a total depth $D = 10$ cm and a cross sectional area $A = 100$ cm², for a total volume of 1 liter. This is an unusually large tumor. If the tumor is located at an average depth of about 20 cm, then $\sigma_{MS} \approx 0.5$ cm, and

$$N_{SKIN} \approx 184 f \quad (25)$$

The number of pixels in the core of each layer is insignificant by comparison to the number in the skin if

$$M \gg \sqrt{\frac{2.2}{f}} \quad (26)$$

This shows that not much dynamic range in pixel size is needed, even for the largest tumors.

Figure 3 shows that it is possible to space the energy layers by as much as $\Delta = 0.7$ cm at an average depth of about 20 cm, while still maintaining 1% cumulative dose flatness. This maximum spacing Δ is relatively insensitive to the required dose flatness, and so there is little advantage in relaxing it (in this calculation) to values like 3% or more that are currently commonplace in practice. Thus there are about $N_E = 14$ energy layers. A grand total of about

$$N_{TOT} \approx 2600 f \quad (27)$$

voxels, or control points, are needed in total.

If the height, width, and depth of the tumor scale together, then the number of voxels scales with the volume V like

$$N_{TOT} \sim V^{2/3} \quad (28)$$

For example, a more typical tumor with a volume of 125 cc requires approximately

$$N_{TOT} \approx 650 f \quad (29)$$

voxels, or control points, in total.

VI. CONCLUSIONS

For a simple model of a tumor shaped like a prism, about 1,000 independent control points are needed to perform the sharpest possible stereotactic surgery, limited only by the physics of proton interactions with matter, with 1% integrated dose flatness. This assumes that a modest adjustment of the lateral size of the beam at the tumor is possible, so that the edges of the tumor receive the sharpest possible beam distributions. While the approach and the results presented here have implications for hardware and software optimization, their exploration is left to other authors and other papers.

ACKNOWLEDGMENTS

Many thanks go to all the members of the RCMS and PCT collaborations, and to T. Bohringer, A. Lomax, E. Pedroni, and U. Schneider.

REFERENCES

- [1] M. Goitein, A. Lomax, E. Pedroni, *Treating Cancer with Protons*, Physics Today, Vol.55 No. 9 pp 45-50, September 2002.
- [2] E. Pedroni et al., "The PSI Proton Therapy Facility" home page http://radmed.web.psi.ch/asm/gantry/gantry_master.html
- [3] T. Satogata et al, *Dose and Sensitivity in Proton Computed Tomography*, C-A/AP/120, Brookhaven National Laboratory, Upton, NY, November 2003. Presented at NSS/MIC 2003, Portland, Oregon. http://www.rhichome.bnl.gov/AP/ap_notes/cad_ap_index.html
- [4] T. Satogata, *The PINT Proton Therapy Simulation Code*, C-A/AP/137, Brookhaven National Laboratory, Upton, NY, February 2004. http://www.rhichome.bnl.gov/AP/ap_notes/cad_ap_index.html
- [5] D.H. Perkins, *Introduction to High Energy Physics*, 4th ed. New York, Cambridge University Press, 2000.
- [6] C. Gardner, S. Peggs, (editors), *Conceptual Design of the RCMS*, Internal technical note, Brookhaven National Laboratory, Upton, NY, 2003.